3B2v7.51c GML4.3.1 NIMA : 20109 Prod.Type:COM pp.1–9(col.fig.:NIL) ED:VijayaT PAGN: VS SCAN: MANGALA

ARTICLE IN PRESS

ELSEVIER

Available online at www.sciencedirect.com

SCIENCE DIRECT®

Nuclear Instruments and Methods in Physics Research A ▮ (▮▮▮▮) ▮▮▮–▮▮▮

NUCLEAR INSTRUMENTS & METHODS IN PHYSICS RESEARCH Section A

www.elsevier.com/locate/nima

High-resolution pixel detectors for second generation digital mammography☆

Tümay O. Tümer[a,*], Shi Yin[a], Victoria Cajipe[a], Henry Flores[a], James Mainprize[b], Gord Mawdsley[b], John A. Rowlands[b], Martin J. Yaffe[b], Eli E. Gordon[c], William J. Hamilton[c], David Rhiger[c], Safa O. Kasap[d], Paul Sellin[e], Kanai S. Shah[f]

[a] *NOVA R&D, Inc., 1525 Third Street, Suite C, Riverside, CA 92507, USA*

[b] *University of Toronto Sunnybrook and Women's College Health Sciences Centre, 2075 Bayview Ave., Toronto, Ont., Canada, M4N 3M5*

[c] *Raytheon Systems Co., 75 Coromar Drive, Goleta, CA 93117, USA*

[d] *Department of Electrical Engineering, University of Saskatchewan, 57 Campus Drive, Saskatoon, Sask., Canada, S7N 5A9*

[e] *Department of Physics, University of Surrey, Guildford, GU2 7XH, UK*

[f] *Radiation Monitoring Devices, Inc., Watertown, MA 02172, USA*

Abstract

Hybrid CdZnTe, CdTe, GaAs, selenium and PbI_2 pixel detector arrays with $50 \times 50\,\mu m^2$ pixel sizes that convert X-rays directly into charge signals are under development at NOVA for application to digital mammography. These detectors have superior X-ray quantum efficiency compared to either emulsion-based film, phosphor-based detectors or other low-Z, solid-state detectors such as silicon. During this work, CdZnTe and CdTe pixel detectors gave the best results. The other detectors are at very early stages of development and need significant improvement. Among other detectors, selenium is showing the highest potential. The preliminary results show that single crystal CdZnTe detectors yield better results in Detective Quantum Efficiency (DQE) as well as in images obtained from phantoms, compared to the polycrystalline CdZnTe detectors. This is due to the non-uniformities in the polycrystaline CdZnTe that degrade the charge transport properties. In this paper, preliminary results from thin (0.15 to 0.2 mm) CdZnTe and CdTe detectors will be presented in terms of MTF, DQE and phantom images. Because of the charge-coupling limitation of the readout Application Specific Integrated Circuit (ASIC) that was originally designed for Si detectors, the detector is biased to collect holes from the input. This charge collection mode limits the CdZnTe detector performance. Their DQE measurements yield 25% and 65% for the polycrystal and single-crystal CdZnTe detectors, respectively. Polycrystal CdTe test detectors were also hybridized to the same type charge readout chip. Since CdTe has much longer hole-propagation lengths compared to CdZnTe, it shows better performance in the hole-collecting mode. However, it suffers from polarization. Excellent images were also obtained from the CdTe detectors. Future work to redesign the readout ASIC and thus improve the detector performance will be discussed. These detectors can also be used for other medical radiography with increased thickness and also for industrial imaging such as non-destructive evaluation and non-destructive inspection.

☆Various sections of this work is separately supported by the following grants: DOD/DAMD17-97-1-7255, NIH/1R43CA80399-02, DoD/DAMD17-99-1-9338, NIH/R01CA84439-01. Without their gracious support this work could not have been achieved.

*Corresponding author. Tel.: +1-909-781-7332.

E-mail address: tumay.tumer@novarad.com (T.O. Tümer).

0168-9002/02/$ - see front matter © 2002 Published by Elsevier Science B.V.

PII: S0168-9002(02)01888-0

Keywords: Breast imaging; Breast cancer screening; Digital mammography; Digital mammography detectors; Pixel detectors; Hybrid pixel detectors

1. Introduction

Digital mammography offers the potential for improved image quality and the possibility of increased performance of detecting breast cancer, particularly in women with dense breasts where current screen-film mammography is often lacking. Digital mammography will also facilitate the implementation of file archiving and retrieving, Computer Aided Diagnosis (CAD) and tele-mammography [1]. Conventional X-ray film mammograms are still an effective way for screening of breast cancer, but its response to X-rays is non-linear and the efficiency is low. Currently, there are phosphor- or scintillator-based CCD or TFT digital mammography systems are available from two manufacturers, but they are less efficient compared to the direct conversion detectors due to the intermediate X-ray to light conversion process [2].

In our earlier work, 1.5 mm silicon and 2 mm CdZnTe detectors were fabricated and tested using a CCD and indium bump bonding technology [3]. Preliminary images were obtained which showed reasonably good spatial resolution and efficiency. Even though Si detectors have the advantage of easy fabrication with low cost, its low atomic number ($Z = 14$) has the disadvantage of low X-ray absorption and thus thick materials are needed to achieve higher sensitivity and contrast. Because thick Si detectors causes angle blurring due to the fan X-ray beam as well as fabrication complications (larger than 1.5 mm thickness is not feasible at present), we then turned our attention to higher atomic number detector materials, such as CdZnTe ($Z = 48$, 30, 52 with only $\approx$10% Zn), CdTe ($Z = 48$, 52), GaAs ($Z = 31$, 33), selenium ($Z = 34$) and PbI_2 ($Z = 82$,53) for developing commercially viable direct conversion digital mammography sensor arrays.

An X-ray imaging system performance can be characterized quantitatively using two measurable parameters: Modulation Transfer Function (MTF) and Detective Quantum Efficiency (DQE). The MTF measures the imaging system's spatial resolution, and the DQE measures the system's efficiency in transferring the signal-to-noise ratio (squared) contained in the incident X-ray pattern to the detector output [4].

In this work, CdZnTe and CdTe solid-state detectors are used to convert the incident X-ray photons directly into electron–hole (e–h) pairs. The created e–h pairs drift in opposite directions toward the electrodes, and charge is generated on the pixel pads at the front end of the detector. The application of bias voltage causes the charged electrons and holes to move in columns and there is negligible charge diffusion into adjacent pixels. This allows the detector thickness to be made much larger than in detectors which have an intermediate light production stage. The charge is then read out by an Application Specific Integrated Circuit (ASIC). A special slot-scan Time Delayed Integration (TDI) technique is used in the readout chip. This technology has the advantage of both charge integration and large well capacity, which meets the high dynamic range and high spatial resolution required for digital mammography. MTF and DQE measurements of several 0.15–0.2 mm thick CdZnTe and CdTe detectors are analyzed and sample images are presented.

New detector materials such as GaAs, selenium and PbI_2 are also tried. They all showed good potential for X-ray imaging but require significant development because they are at the very early stages of development in this field. For these detectors only preliminary images are presented and detailed measurements of MTF and DQE are not yet carried out. Work on these new detectors, especially selenium pixel detectors, is promising and continuing.

2. Method

An ASIC (MARY™ chip) has been developed at NOVA to meet the readout requirement of the digital mammography hybrid pixel detectors [3]. Because the charge capacity requirement for good image quality exceeds the capabilities of standard chips, this ASIC chip uses a slot-scanning, multi-section TDI technique for dose efficient scatter rejection and the ability to use small detectors to produce a large area image. The MARY chip consists of 24 independent sections, each section uses CCD technique with 8 rows for charge transfer in TDI mode. The signal from each section is combined off-chip to produce a full signal image. This chip is a good test platform where various X-ray detectors can be indium bump bonded on for testing. A p-channel process was used in the fabrication of the MARY chip and therefore it carries holes in its CCD wells, which is best suited for some of the detectors such as Si, GaAs and selenium. However, in other detectors, especially CdZnTe and CdTe holes are readily trapped. Therefore, a modified version of the MARY ASIC with negative input, suitable for reading out electrons, is required.

The CdZnTe, CdTe and GaAs detectors are fabricated using the following steps. First, the detector material is prepared, polished and an array of two-dimensional pixelated electrodes are deposited on the surface [3,4]. Then the detectors are indium bump bonded onto the readout ASIC. The detector and the ASIC have matching pixel dimensions and geometry. The CdZnTe and CdTe pixel detectors are then trimmed down, using a proprietary Diamond Point Turning (DPT) technique, to a small thickness of the order of 0.15–0.2 mm without degrading the detector's spectroscopic properties, to allow the collection of holes by ASIC. We have compared the ^{241}Am spectrum of a commercial pad detector to that of a DPT processed detector, and found no difference in their spectra where both detectors yield a 7% energy resolution of the 60 keV photo peak [10].

The MTF and DQE are measured in an X-ray system for mammography where the X-ray target is 40 cm away from the detector. A tantalum edge is translated across the detector during the X-ray exposure and the pre-sampled MTF is calculated using an over-sampled edge technique [2]. Noise properties are assessed using a simulated slit calculation on a flat-fielded image of a 6-mm thick PMMA slab. From these data and the measured radiation exposure, the DQE of the imaging system is calculated [2].

For the polarization measurements, similar flat-fielded images are taken as described above, and the signal strengths are calculated after each X-ray exposure. The initial measurement is normalized to one for comparison with different detectors or test setups.

Samples are scanned under a computer-controlled step-motor, with the scanning speed optimized for synchronization with the charge transfer speed inside the readout chip. Simple image processing techniques, such as background subtraction, gain calibration and contrast maximization are applied to images acquired in the test.

3. Results

3.1. MTF and DQE

The MTF has been measured for a 0.2 mm thick CdZnTe detector. Fig. 1 shows an MTF plot from the detector. The Nyquist frequency limit for this detector is 10 lp/mm, and we have obtained 25% in MTF at 10 lp/mm. Since we adopt a slot scanning technique, the MTF values in the slot (non-scanning) direction are always better than those in the scanning direction, due to the temporal blurring caused by the movement of the scanning arm. In the MTF and DQE plots, we also include the theoretical simulation curves both in the slot and scan directions, which are based on earlier theoretical analysis [8,9].

Because of the charge polarity of our present MARY readout chip (p-channel), holes were collected for the CdZnTe and CdTe detectors. This configuration causes the charge signal loss in CdZnTe, as discussed earlier.

Fig. 2 shows a DQE plot for a polycrystaline CdZnTe detector, where the DQE is measured to be only about 25% at zero spatial frequency.

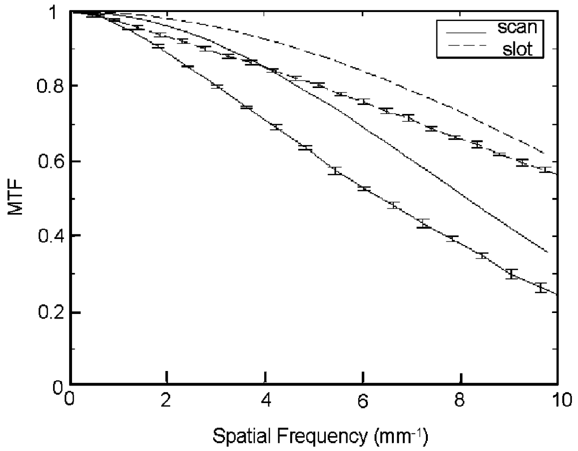

Fig. 1. MTF plots, both theoretical and experimental data, of a 0.2 mm thick polycrystaline CdZnTe detector. The experimental data curves have error bars. The Nyquist limit of this detector is 10 lp/mm.

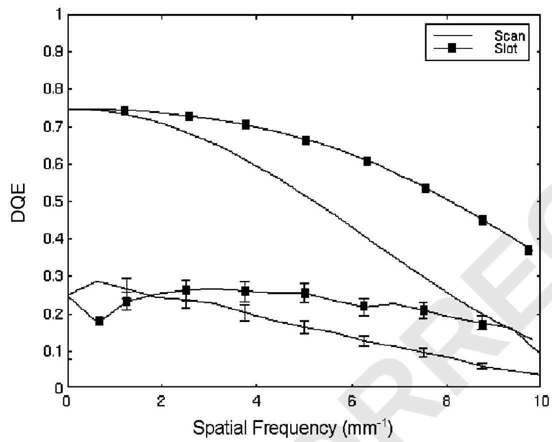

Fig. 2. DQE plots of a 0.2 mm thick polycrystaline CdZnTe detector for both theoretical prediction and experimental data. The measured DQE reaches only about 25% at zero spatial frequency. Curves with filled square are in the slot direction and experimental data have error bars.

When a single crystal CdZnTe detector was used, DQE was significantly improved reaching 65% at zero spatial frequency, as shown in Fig. 3.

In our earlier report [3], the DQE for silicon detectors varied from 55% to 75% at zero spatial frequency. We ascribe the poor DQE values for CdZnTe detectors to the incorrect (positive) charge collection mode, which results in about

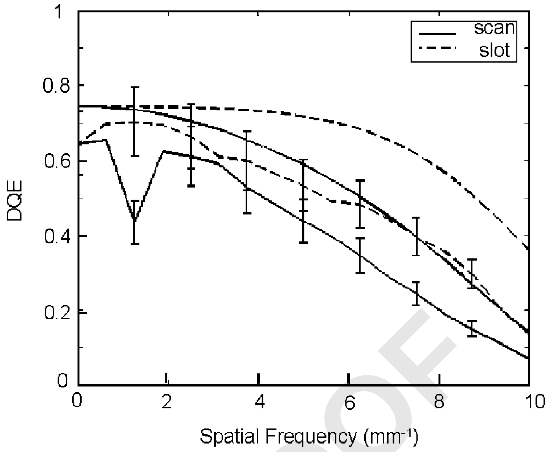

Fig. 3. DQE plots of a 0.15 mm thick single crystal CdZnTe detector. The DQE reaches about 65% at zero spatial frequency. The smooth curves without error bars are the theoretical simulations and the experimental data are shown with error bars on them. Broken lines show the response in the slot direction.

30–60% charge collection loss. We are in progress to design our next version readout chip such that electrons are collected at the input of the readout chip (n-channel). Development of a new MARY ASIC with negative (electron) input instead of holes is expected to improve the DQE significantly by: (1) Decreasing trapping because electrons suffer lees trapping compared to holes and (2) increasing detector thickness. The DQE is expected top approach theoretical limit. Fig. 3 shows the DQE plot of a 0.15 mm thick single crystal CdZnTe detector. Much improved DQE values were obtained, which is probably due to significantly lower trapping of holes inside the detector.

Since CdTe has very similar detector properties compared to CdZnTe, we also fabricated 0.15 mm thick CdTe detectors and indium bump bonded them to our present hole-collecting MARY readout chips. The CdTe material was obtained from Eurorad (Strasbourg). Fig. 4 shows an MTF plot of a CdTe detector, which is similar to that of the CdZnTe detector (Fig. 1). Fig. 5 shows the DQE plot of the 0.15 mm thick CdTe detector, where the DQE at DC reaches only 40%. This low DQE value can be explained by charge collection inefficiency, probably due to the polarization effect.

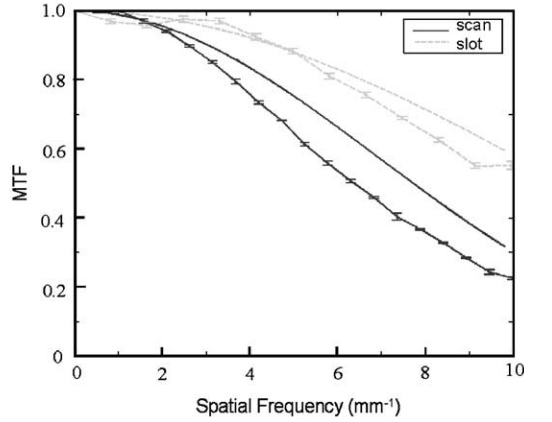

Fig. 4. MTF plot of a 0.15 mm thick polycrystalline CdTe detector. The top two curves are theoretical and experimental data in the slot (non-scanning) direction and the lower two curves are the data obtained in the scanning direction. Again the measured data are shown with error bars.

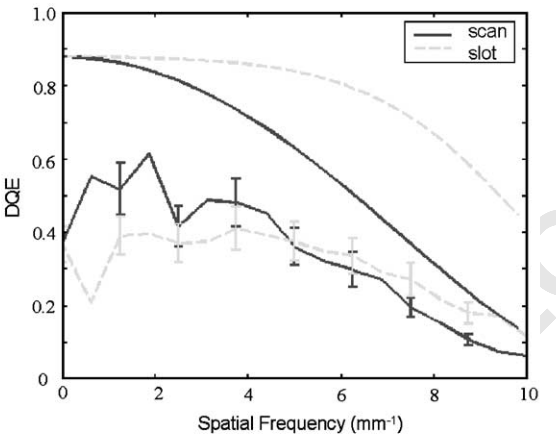

Fig. 5. DQE plot of a 0.15 mm thick polycrystalline CdTe detector at 26 kVp. The detector had polarization effect, which significantly increased the background noise. About 40% DQE is achieved at DC. The smooth curves are the theoretical simulations with broken lines representing the results in the slot direction.

3.2. Polarization effect observed in CdTe pixel detectors

Since the hole-propagation length for CdTe is about 10 times larger than that of CdZnTe, we expect to see improved charge collection efficiency and thus higher DQE for this detector. Fig. 5 shows the DQE measurement results, where the DQE at DC reached only 40%. This low DQE value may be explained by charge collection inefficiency, probably due to the polarization effect. CdTe detectors are known to have polarization effect, where the accumulated charge inside the detector forms an internal field that effectively reduces the external bias field [6,7]. Polarization is a function of detector bias voltage, X-ray flux and temperature. Therefore, some control of the polarization is possible by adjusting these parameters such as increasing bias voltage, lowering flux and/or increasing temperature. In digital mammography, the crucial parameter is the flux, which is high compared to other applications and it is not possible to reduce it significantly due to increase in patient exposure time.

Fig. 6 shows the detector output signal as a function of X-ray exposures. For detector (a), we see about 8% signal drop at X-ray exposures 10 s apart, but the signal drop is less at 5 min X-ray exposure intervals. For detector (b), we see clearly the signal drop, even though the waiting between X-ray exposures is quite long. Results from Fig. 6 suggest that the present CdTe detectors have significant polarization effect, which decreases the charge collection efficiency, and thus causes low DQE measurements. We can also see that this polarization effect has sample dependence. The

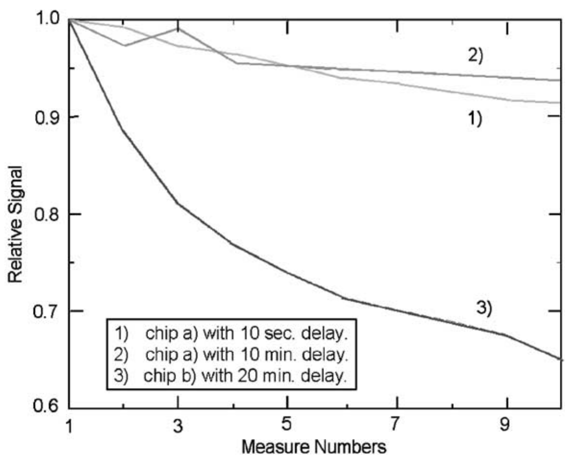

Fig. 6. Output signals vs. number of X-ray exposures for two CdTe detectors. Curves (1) and (2) are measured from detector (a) where curve (1) is at 10 s and (2) is at 10 min X-ray exposure intervals. Curve (3) is from detector (b) where the exposure time interval is about 20 min.

two samples shown in Fig. 6 were made from the same batch of CdTe materials using the same fabrication process, yet their polarization behaviors are different: Sample (b) shows a much lower signal strength. How to increase the yield of detectors with low or negligible polarization remains a challenging task for future application of this material.

Several improvements could be done to reduce the polarization effect in CdTe for application to digital mammography. For the present CdTe material we used, the resistivity was less than $10^9\,\Omega$ cm, and the dark current limited the maximum bias voltage applicable to only several volts. If we can improve the resistivity of the CdTe material, then higher bias voltage can effectively reduce the polarization. A properly designed and implemented metal contact may also improve the polarization [6]. Also the electrons are affected less by polarization and when an electron collection version of the MARY chip is made CdTe pixel detectors may show much less polarization effect. Therefore, CdZnTe with low polarization is the preferred detector material until the resistivity of CdTe can be increased to about $10^{11}\,\Omega$ cm and the polarization is nearly eliminated.

3.3. Image quality

Fig. 7 shows image comparisons of a small mosquito fish taken using a 0.15 mm CdZnTe detector and a 0.15 mm CdTe detector. The top image is obtained using the CdZnTe detector and the bottom image is from the CdTe detector. The fish is about 20 mm in length and we see clear bone structures of the fish in both pictures. The CdTe image seems to have a slightly poorer picture quality than the CdZnTe one, which might be due to the polarization effect in the CdTe material that causes higher background noise.

We have also compared images from silicon and CdZnTe pixel detectors. Fig. 8 shows two images of a finger phantom with real human bone embedded inside. Image on the left is taken using a CdZnTe pixel detector and the image on the right is from a silicon pixel detector. Both use the same MARY readout chip. Although silicon detector thickness was 1 mm, the quality of the image for the CdZnTe pixel detector is much higher. This is because of no angle blurring and the higher DQE achieved with CdZnTe pixel detector, although only holes are collected. The angle blurring in the silicon image is due to the 1 mm thickness of the Si detector. This is because for thick detectors, any tilted incident X-rays will generated the electron–hole pairs along the incidental direction that are not along the field lines and therefore the charge will be deposited over neighboring pixels, causing such a blurring.

We have also imaged the smallest and the least contrast features of the standard mammography test and calibration phantom and compared to the phantom images obtained by a commercial digital mammography system. These images show that our CdZnTe pixel detectors show improved contrast compared to the first generation digital mammography systems. These images again are taken by collecting holes. When the electron

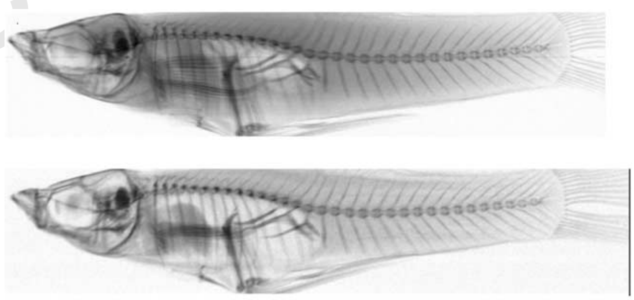

Fig. 7. Two images of a mosquito fish using a 0.15 mm thick CdZnTe detector (top) and a 0.15 mm thick CdTe detector (bottom). The X-ray was set at 30 kVp and 40 mA for both images. The length of the fish is about 20 mm.

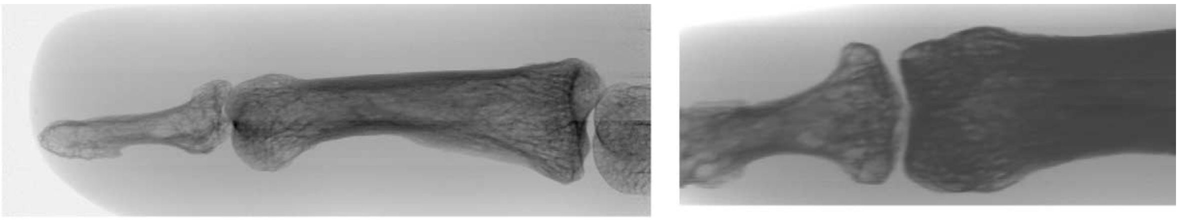

Fig. 8. Images of a human finger phantom from a 0.15 mm thick CdZnTe detector (left) and a 1 mm thick Si detector (right). Detailed bone structures are clearly visible. The CdZnTe detector seems to show a better image than the Si one. The X-ray was set at about 26 kVp and 59 mR, and the images are displayed in log scale.

collecting version of the MARY ASIC is fabricated we expect the contrast in these smallest and faintest features will be further enhanced because of the improvement in the DQE (Fig. 9).

3.4. Other pixel detectors

Fig. 10 shows a new GaAs pixel detector developed and tested at our laboratory. A preliminary image of a patterned metal collimator is shown. The image is effected mainly due to the low depletion thickness as well as strong charge trapping in the present GaAs material. Work on increasing the GaAs depletion thickness, improving charge trapping and detector uniformity is continuing.

Fig. 11 shows the first selenium detector developed together with our collaborators. This detector is not indium bump bonded onto the MARY ASIC. It is directly deposited. This is a new technique we are developing which may eliminate the need for indium bump process. The first prototype developed is showing promising result as seen from the image obtained by this detector on the right-hand side. However, it needs significant work to improve and establish this new technique as a viable detector technology for digital mammography. Fig. 12 shows a preliminary image obtained from a PbI_2 pixel detector fabricated similar to the selenium pixel detector. Again the new detector is giving promising results. However, this is a very new detector material and needs further development before it can be used on our pixel detectors.

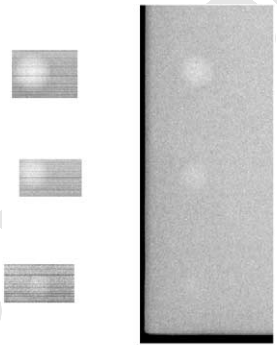

Fig. 9. Phantom image comparison of a CdZnTe detector to that of a commercial first-generation digital mammography unit. The phantom is the standard mammographic model RMI 156 with only the wax insert. On the right: a partial phantom image is shown obtained from a commercial digital mammogram unit. On the left: images obtained using our CdZnTe detector at NOVA. The three disks are feature numbers 14, 15, and 16 in the phantom.

4. Discussion and summary

Our test results and numerous images show that CdZnTe and CdTe are excellent materials for X-ray imaging and second-generation direct conversion digital mammography. Excellent results are obtained for both materials. Due to the MARY readout chip limitation at present, holes are collected for these detectors. The CdTe detectors have longer hole-propagation lengths, which improve hole collection efficiency. However, polarization effect reduces its performance. Improved detector resistivity and/or contact metalization may reduce this effect. To utilize the maximum potential of the CdZnTe detector, an electron (negative) input version of the MARY readout

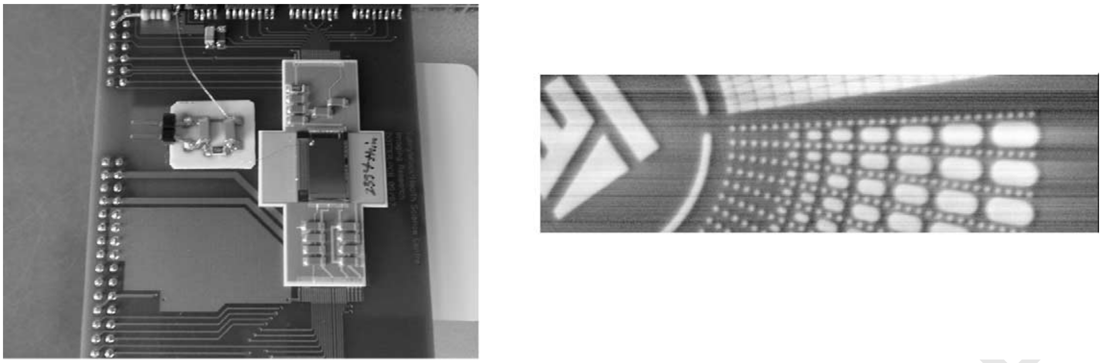

Fig. 10. A GaAs pixel detector hybrid is mounted on a daughter card. The thickness of the GaAs detector is 0.15 mm. The X-ray is set at 39 kVp and 32 mA. The Bias is set at 6 V. This is a small size detector that has a 192×128 pixel array. On the right an image of a patterned metal collimator obtained using this pixel detector.

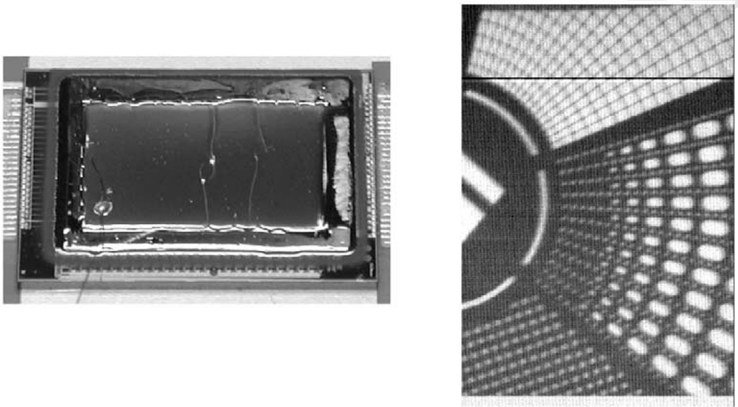

Fig. 11. The selenium pixel detector with 0.125 mm Se deposited on top of a MARY ASIC. The X-ray is set at 39 kVp and 32 mA. The bias is set at 200 V. The $\mu-\tau$ product for holes in this material is $1.9 \times 10^{-5}\,\mathrm{cm^2/V}$ [5]. The $\mu-\tau$ product for electrons in this material is $9.1 \times 10^{-7}\,\mathrm{cm^2/V}$ [5]. The image of a fine mash metal collimator is shown on the right.

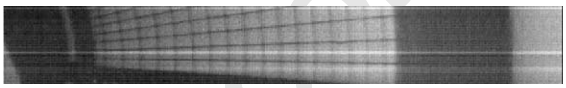

Fig. 12. Image of a metal collimator pattern from a PbI2 detector. The PbI2 material is directly deposited onto a MARY readout chip similar to Fig. 11, with 70 μm in thickness. The detector is biased at 50 V. The X-ray is set at 39 kVp and 32 mA.

chip is necessary to maximize the charge collection efficiency. This will produce better DQE than those presented here.

We have demonstrated that the measured DQE for the CdTe and CdZnTe detectors reached 40% and 60%, respectively. These detectors have potential for higher DQE with improved fabrication technique and using an optimized readout ASIC. These values are superior than those from screen films or scintillator-based digital mammography systems, which are typically around 30–40% [2]. A major task for the future is to redesign the MARY readout chip with negative input. A multi-detector linear sensor array about 20–25 cm long is also under construction where full breast size images could be obtained. Because a linear array with about 1 cm width is used, scattered X-ray background will be very low, thus eliminating the need for the grid [2,3]. This, together with high

DQE, can help reduce the patient doze by up to a factor of 6.

A high contrast and high-resolution digital mammography system will help reduce the false negative and false positive detection rates in current mammograms. This will reduce mortality and unnecessary and traumatic biopsies for women. Lower dose can increase safety and reduce screening intervals, thus improving early detection. Increased contrast can save lives of female patients who have dense breasts.

The present slot-scanning detector system can easily be applied to other medical imaging applications such as digital radiography, if the detector thickness is carefully selected to stop the energy range required. The direct conversion technique allows the increase in detector thickness without significant effect on the spatial resolution. The pixel detectors under development can also be applied to industrial imaging such as Non-Destructive Evaluation (NDE) and Non-Destructive Inspection (NDI). The TDI technique is highly suitable for conveyer belt-type scanning where the detectors can be mounted onto the conveyer belt and the products can be imaged in real time. Since industrial imaging does not need stringent requirements like medical imaging, the cost of detector manufacture and calibration can be significantly less. Also silicon pixel sensor array-based systems can be used for low-energy X-ray imaging applications with much reduced cost and the CdZnTe or CdTe detectors can be applied for critical imaging applications where higher energy X-ray imaging and/or higher contrast is required.

References

[1] S.A. Feig, M.J. Yaffe, Digital mammography, computer-aided diagnosis, and telemamography, Radiological Clinics of North America 33 (1995) 1205.

[2] N.L. Ford, J.G. Mainprize, S. Yin, T.O. Tümer, E.E. Gordon, W.J. Hamilton, M.J. Yaffe, Comparison of different detector materials for digital mammography, Proceedings of the Fifth International Workshop on Digital Mammography, Toronto, Canada, June 11–14, 2000, p. 39.

[3] S. Yin, T.O. Tümer, D. Maeding, J. Mainprize, G. Mawdsley, M.J. Yaffe, W.J. Hamilton, Direct conversion detectors for digital mammography, IEEE Tranc. Nucl. Sci. NS-46 (6) (1999) 2093–2097.

[4] M.J. Yaffe, J.A. Rowlands, X-ray detectors for digital radiography, Phys. Med. Biol. 42 (1997) 1.

[5] C. Szeles, E.E. Eissler, D.J. Reese, S.E. Cameron, Radiation detector performance of CdTe single crystal grown by the conventional vertical Bridgman technique, SPIE Proc. 3768 (1999) 98.

[6] R.O. Bell, G. Entini, H.B. Serreze, Time-dependent polarization of CdTe gamma-ray detectors, Nucl. Instr. and Meth. 117 (1974) 267.

[7] H.L. Malm, M. Martini, Polarization phenomena in CdTe: preliminary results, Can. J. Phys. 51 (1973) 2336.

[8] J.G. Mainprize , M.J. Yaffe, T.O. Tümer, S. Yin, W.J. Hamilton, Design considerations for a CdZnTe digital mammography system, Proceedings of the Fourth International Workshop on Digital Mammography, Nijmegen, 1998, pp. 19–26.

[9] J.G. Mainprize, N.L. Ford, S.Yin Nancy, T.O. Tümer, M.J. Yaffe, Image quality of a prototype direct conversion detector for digital mammography, Proc. SPIE 3659 (1999) 398.

[10] Shi Yin, T.O. Tümer, D. Maeding, J. Mainprize, G. Mawdsley, M.J. Yaffe, E.E. Gordon, W.J. Hamilton, Direct conversion CdZnTe and CdTe detectors for digital mammography, IEEE Transc. Nucl. Sci., 2001, accepted for publication.